NASA TECHNICAL NOTE

NASA TN D-6148

c.1

NASA TN D-6148

EFFECT OF SURFACE PREPARATION ON OXIDATION OF WI-52 AT 1800° AND 2000° F (1255 AND 1366 K)

by Carl E. Lowell and Isadore L. Drell

Lewis Research Center
Cleveland, Ohio 44135

NATIONAL AERONAUTICS AND SPACE ADMINISTRATION • WASHINGTON, D. C. • FEBRUARY 1971

1. Report No.
NASA TN D-6148

2. Government Accession No.

3. Recipient's Catalog No.

4. Title and Subtitle
EFFECT OF SURFACE PREPARATION ON OXIDATION OF WI-52 AT 1800° AND 2000° F (1255 AND 1366 K)

5. Report Date
February 1971

6. Performing Organization Code

7. Author(s)
Carl E. Lowell and Isadore L. Drell

8. Performing Organization Report No.
E-5668

9. Performing Organization Name and Address
Lewis Research Center
National Aeronautics and Space Administration
Cleveland, Ohio 44135

10. Work Unit No.
129-03

11. Contract or Grant No.

12. Sponsoring Agency Name and Address
National Aeronautics and Space Administration
Washington, D.C. 20546

13. Type of Report and Period Covered
Technical Note

14. Sponsoring Agency Code

15. Supplementary Notes

16. Abstract

High-temperature X-ray diffraction, high-temperature microscopy, and weight-gain experiments were combined to investigate the effect of surface preparation on the static-air oxidation of WI-52, a cobalt-base superalloy. Surface preparation was found to affect the order, relative amounts, and morphology of the oxides formed. Oxidation at 1800° F (1255 K) for 100 hours caused weight gains in ground-and-lapped specimens that were four times that of metallographically polished specimens. Upon cooling, only the ground-and-lapped specimens spalled. Models of oxidation were developed to describe the surface-preparation effects.

17. Key Words (Suggested by Author(s))
Oxidation; Cobalt; Superalloy; WI-52; Oxides; Surface-preparation; X-ray-diffraction; High-temperature metallography

18. Distribution Statement
Unclassified - unlimited

19. Security Classif. (of this report)	20. Security Classif. (of this page)	21. No. of Pages	22. Price*
Unclassified	Unclassified	32	$3.00

*For sale by the National Technical Information Service, Springfield, Virginia 22151

EFFECT OF SURFACE PREPARATION ON OXIDATION OF WI-52 AT 1800° AND 2000° F (1255 AND 1366 K)

by Carl E. Lowell and Isadore L. Drell

Lewis Research Center

SUMMARY

High-temperature X-ray diffraction, high-temperature microscopy, and weight-gain experiments were combined in an attempt to understand the static-air oxidation of a cobalt-base superalloy, WI-52, at 1800° and 2000° F (1255 and 1366 K). Surface preparation was a variable. It was found to have a pronounced effect on the oxidation process even after 100 hours exposure. This variable affected not only the order, relative amounts, and morphology of the oxides formed but also the total weight gained.

Metallographically polished surfaces were found to oxidize at the lowest rates. The rates were similar to those found for Co-Cr alloys with the same Cr content as WI-52. Gound-and-lapped surfaces oxidized faster, and at 1800° F (1255 K) showed a sudden increase in weight for part of the 100 hours, resulting in a total weight gain four times that of the polished specimens. Upon cooling, only the ground-and-lapped specimens spalled. These differences were related to a change in the major oxides in the scale. Models of oxidation were developed to describe the mode of oxidation with differing surface preparations.

INTRODUCTION

One of the superalloys currently used in jet engines for stator vanes is WI-52. It is used for its high-temperature strength and resistance to thermal fatigue. Its usefulness is limited, however, by its lack of good oxidation resistance at high temperatures. Little prior work has been done on the oxidation resistance of WI-52. That which has is limited primarily to weight-gain experiments (refs. 1 and 2).

Because of the importance of this alloy to jet engine technology, this study was undertaken in an attempt to understand the oxidation behavior of WI-52 and how it is affected by surface preparation. The oxidation temperatures covered by this work were 1800° and 2000° F (1255 and 1366 K).

One problem arises immediately. Superalloys are complex and undergo complex oxidation processes. Reliance on one or two techniques to evaluate such oxidation behavior is not sufficient. The work described below was an attempt to understand WI-52 oxidation behavior by bringing as many techniques to bear on the problem as possible. Among these techniques were room-temperature X-ray diffraction (XRD); X-ray fluorescence (XRF); electron microprobe (EMP); high-temperature metallography (HTM); room-temperature metallography; gravimetric analysis (ΔW); and high-temperature X-ray diffraction (HTXRD), which was previously reported (ref. 3). An attempt has been made to correlate the data obtained from these techniques and to describe a model for the oxidation processes present.

MATERIALS AND PREPARATION

WI-52 was obtained as a cast alloy in coupons 1 inch (2.54 cm) by 2 inches (5.08 cm) by 0.1 inch (0.25 cm). The chemical analysis in table I shows that this alloy is basically Co-20Cr-10W-2Nb-2Fe (cobalt - 20 percent chromium - 10 percent tungsten - 2 percent niobium - 2 percent iron). The microstructure is shown in figures 1(a) and (b). By a

TABLE I. - ANALYSIS

OF WI-52

Element	Heat 220	Heat 219
	Weight percent	
Co	Balance	Balance
Cr	21.15	21.60
W	11.2	11.1
Nb[a]	1.73	1.77
Fe	2.10	2.14
C	.47	.47
Ni	.39	.42
Mn	.27	.28
Si	.27	.34
S	.017	.016
P	.015	.014

[a] Absence of possible Ta in wet chemistry analysis shown by X-ray fluorescence.

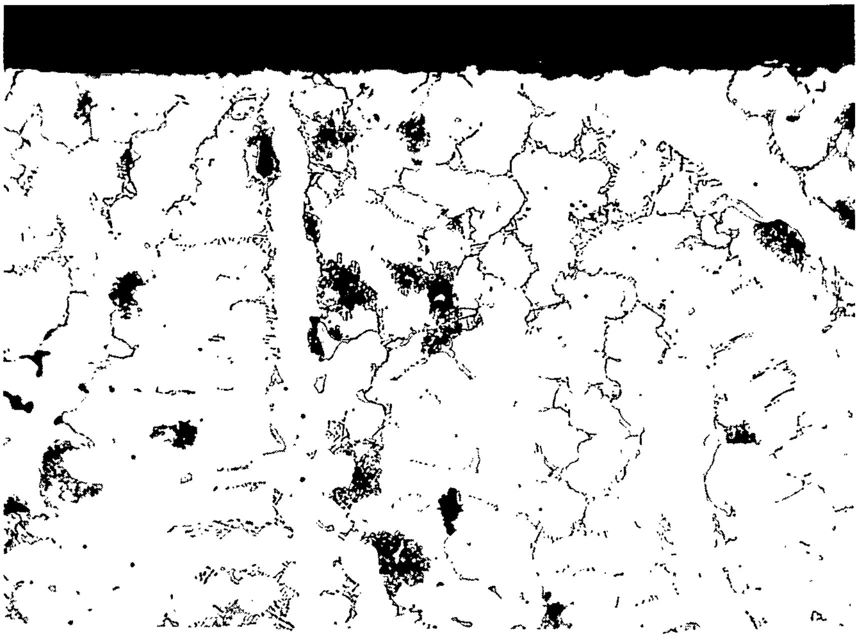

(a) As polished. X250.

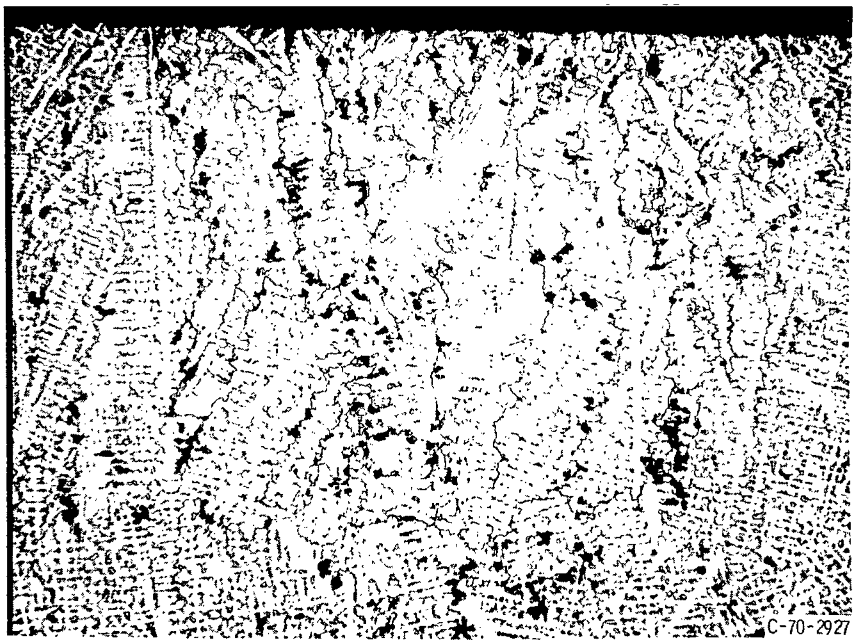

(b) Etched with 30 percent oxalic acid, 70 percent H_2SO_4. X50.

Figure 1. - Microstructure of as-cast WI-52. Platelets or needles are (Nb, W)C, irregular grey phase is M_6C, matrix is cobalt solid solution.

combination of XRD, XRF, and EMP on both the as-cast material and electrolytic extractions, the matrix was identified as a cobalt solid solution with carbides at the grain boundaries. There are at least two carbides: (Nb,W)C and $(Cr, W, Co)_6C$. The (Nb, W)C predominates in the form of needles or platelets, while the $(Cr, W, Co)_6C$ appears as irregularly shaped particles. These carbides were identified by XRD after separation by chemical digestion. Figure 1(b), which shows WI-52 etched, indicates some coring present from the casting.

There were four types of surface finishes used in the program: surface grinding with a rubber-bonded SiC wheel, grinding followed by lapping with 20-micrometer diamond paste, metallographic polishing through 0.5-micrometer diamond paste, and electropolishing in an electrolyte of 77 percent glacial acetic acid - 23 percent perchloric acid. All surfaces except those ground and lapped had rms finishes of 1 to 3 microinches (0.025 to 0.075 μm). The ground-and-lapped surface roughnesses were 10 to 20 microinches (0.25 to 0.50 μm). Samples for HTXRD (ref. 3) were cut to 0.95- by 1.27-centimeter slabs. The HTM samples were cut to 0.6-centimeter-diameter disks. The ΔW samples were cut to 2.54- by 1.90-centimeter slabs. All samples were thinned only through surface preparation.

EQUIPMENT AND PROCEDURES

Gravimetric Analysis (ΔW)

The weight-gain apparatus is shown in figure 2. The specimens, after preparation, were suspended above the furnace from one pan of the balance. Weights were added to the other pan to attain a null reading. After the temperature of the furnace was stabilized at the oxidation temperature, the furnace was raised to position the sample in the center of the hot zone. The recorder was then started and remained on for the duration of the 100-hour runs to record ΔW. The accuracy of the recorded weights was ±0.5 milligram. After an initial 18° F (10 K) drop when the furnace was raised, the hold temperature was regained in less than 10 minutes. The temperature remained constant from then on within ±4° F (±2 K). The airflow was by convection only.

At the end of a run, the furnace was lowered and a pyrex beaker placed around the oxidized specimen to catch possible spall. Some samples were "potted," that is, transferred immediately upon emergence from the furnace into a low-melting lead alloy for retention of the scale of samples which might otherwise spall.

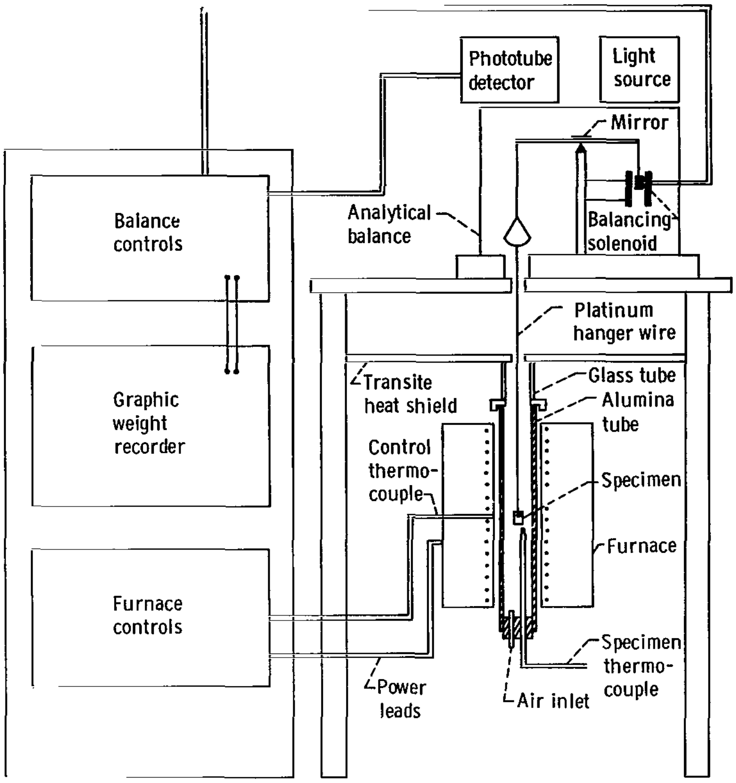

Figure 2. - Continous-weight-gain apparatus.

High-Temperature X-Ray Diffraction (HTXRD)

The HTXRD setup has been described previously (ref. 3). Briefly, the specimen (fig. 3), which rests on a platinum heater with a platinum/platinum-13-percent-rhodium thermocouple spot-welded to the surface struck by the X-ray beam, is heated to the oxidation temperature in static air. Diffractograms are taken at intervals throughout the course of approximately 100 hours. Data from the diffraction patterns are plotted as the peak intensities of the major diffraction lines of the various oxide phases against time. At the conclusion of the run, patterns were also taken at several temperatures between the oxidation temperature and room temperature during cooling.

Room-Temperature X-Ray Diffraction and X-Ray Fluorescence (XRD and XRF)

The XRD of the oxide scales was obtained using 114.6-millimeter-diameter Debye cameras. Copper or chromium Kα radiation was used. Samples were prepared by

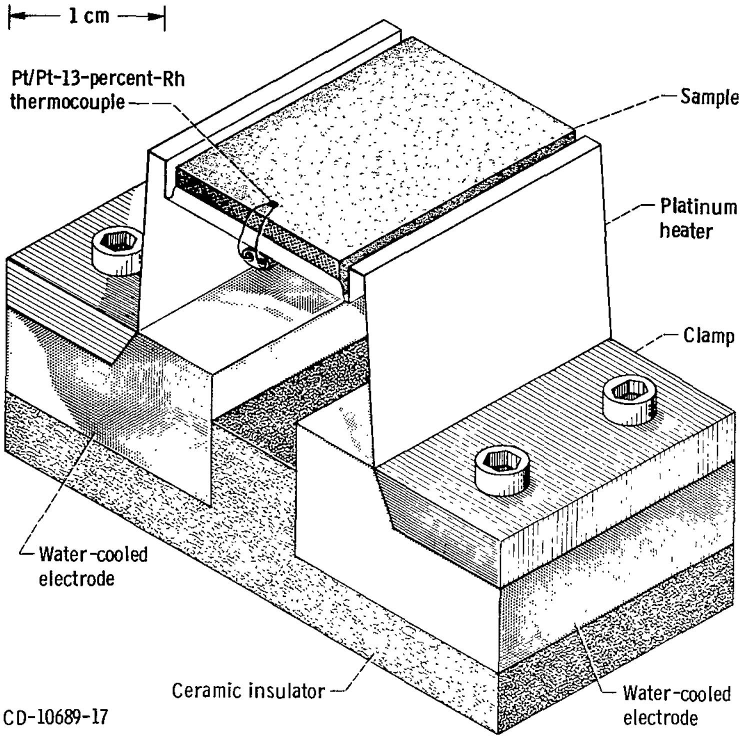

Figure 3. - Detail of heater-sample arrangement for high-temperature X-ray diffraction.

either grinding of spalls or scraping the retained scale with a diamond tool. The XRF utilized a gold-target X-ray tube for excitation and a lithium fluoride (LiF) analyzing crystal. Sample preparation was generally as in XRD. Some sample surfaces, however, were run without treatment.

Room-Temperature Metallography

Light-metallography examination of the oxidized surfaces and the sample cross section were made both in bright field and under polarized light. Polarized light was tried in an effort to use color as an aid in identifying the scale layers.

Electron-metallography techniques were used both to study the morphology of the initial oxide growth and to extract, by replication, some of the initial oxidation products. The brittle oxide broke off and became embedded in the replica of 0.25-percent Movital and parlodion. Enough of these particles were retained in the replica to allow electron diffraction.

High-Temperature Metallography (HTM)

Figure 4 is a schematic diagram of the HTM apparatus. The objective, which throughout this work was ×10, was specially corrected for use through the quartz plate. Magnification on final prints is ×250. The plate protected the objective from condensation of vapors coming from the oxidizing surface of the sample. The plate was movable to allow transmission through a clean area after contamination by condensates at the original viewing area. Incidient bright-field illumination was used throughout. The image was recorded primarily on medium-speed black-and-white film; the camera magazine held 250 exposures. The black-and-white exposures were activated by an intervalometer. This instrument could adjust the exposure intervals from 1 second to 10 hours. Some 16-millimeter color motion-picture footage was taken to ensure continuity.

The schedule of operation was as follows: After polishing (this and a 320-grit abrasion were the only surface preparations used with this apparatus), the sample was placed on the heater. Simultaneously, the sample was raised to the oxidation temperature, typically in 30 seconds, and exposures were started at the rate of one frame per 4 seconds. After a few minutes, the rate was slowed gradually to one frame per 15 minutes. At the end of a run, the sample was cooled rapidly to room temperature.

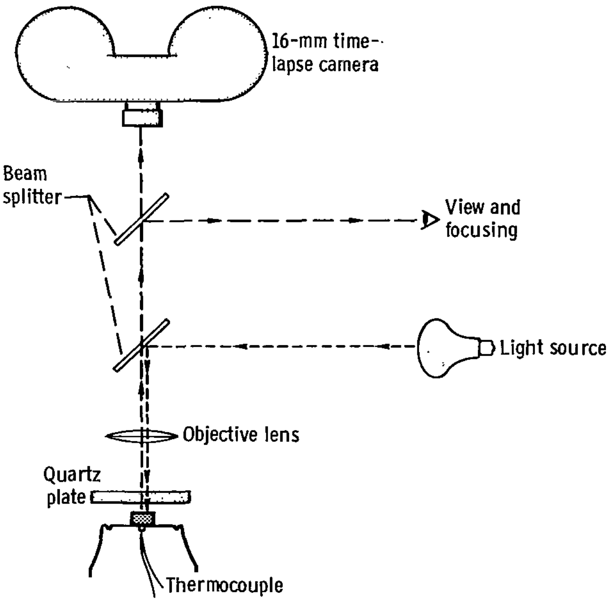

Figure 4. - High-temperature microscope.

RESULTS AND DISCUSSION

Gravimetric Analysis (ΔW)

The results of the weight-gain experiments are plotted as the square of the weight-gain per unit area in figures 5 and 6. Use of these square plots is not meant to imply that the oxidation is parabolic. Interpreted in terms of the usual models of oxidation, parabolic kinetics would suggest oxidation controlled by diffusion through a uniform oxide layer. A multiphase alloy like WI-52 could hardly form such a layer except in patches (see HTM section). At best, parabolic behavior could only be approximated. However, square plots are useful to compare the data obtained with that of related alloys (refs. 2, and 4 to 7).

At 1800° F (1255 K), the oxidation behavior of electropolished and metallographically polished samples appears to be relatively uncomplicated. Both square plots are linear throughout and have nearly the same slope, 0.017 $mg^2/(cm^4)(hr)$. This slope is quite close to that obtained by Phalnikar, Evans, and Baldwin (ref. 7) for binary Co-Cr alloys with the same Cr content as WI-52. However, for the same Co-Cr alloy, Kofstad and Hed (ref. 5) found a slope about 50 times greater. It is possible that the differences in slope measured by Phalnikar and Kofstad are due to impurities in the materials, but unfortunately neither investigator presents his analysis, so comparison is not possible. This is of considerable interest since if Phalnikar's data represent the Co-Cr system, the addition of tungsten, manganese, nickel, iron, and silicon to the solid solution has little effect on the oxidation rate. If, however, Kofstad's data from a sample of the same surface preparation are used for comparison, these additions reduce the oxidation rate by more than 50 times.

The introduction of stress or roughness into the sample surface affects the oxidation rate unfavorably. Surface grinding increases the rate by a factor of 2 for the first 50 hours, 0.037 $mg^2/(cm^4)(hr)$, after which the rate nearly doubles again to 0.068 $mg^2/(cm^4)(hr)$. A more peculiar curve is obtained by grinding and lapping. The curve has three distinct portions and is analogous to those found by Wolf and Sandrock (ref. 4) for L-605, a cobalt-base alloy similar to WI-52 but containing more tungsten (15 compared to 11 percent). The ground-and-lapped sample came from the same coupon as the metallographically polished sample, making compositional differences an unlikely cause for the oxidation differences. Composition differences were suggested by Wolf and Sandrock for the "anomalous weight increment." Also pertinent is the fact that Douglass and Armijo (ref. 2) found this peculiarly shaped curve in WI-52 and L-605 when their samples were ground or grit blasted but not when electropolished or vacuum annealed. The initial slope, 0.11 $mg^2/(cm^4)(hr)$, is higher than any of the others; it is more than six times as great as the slope of the curve for the polished sample. From

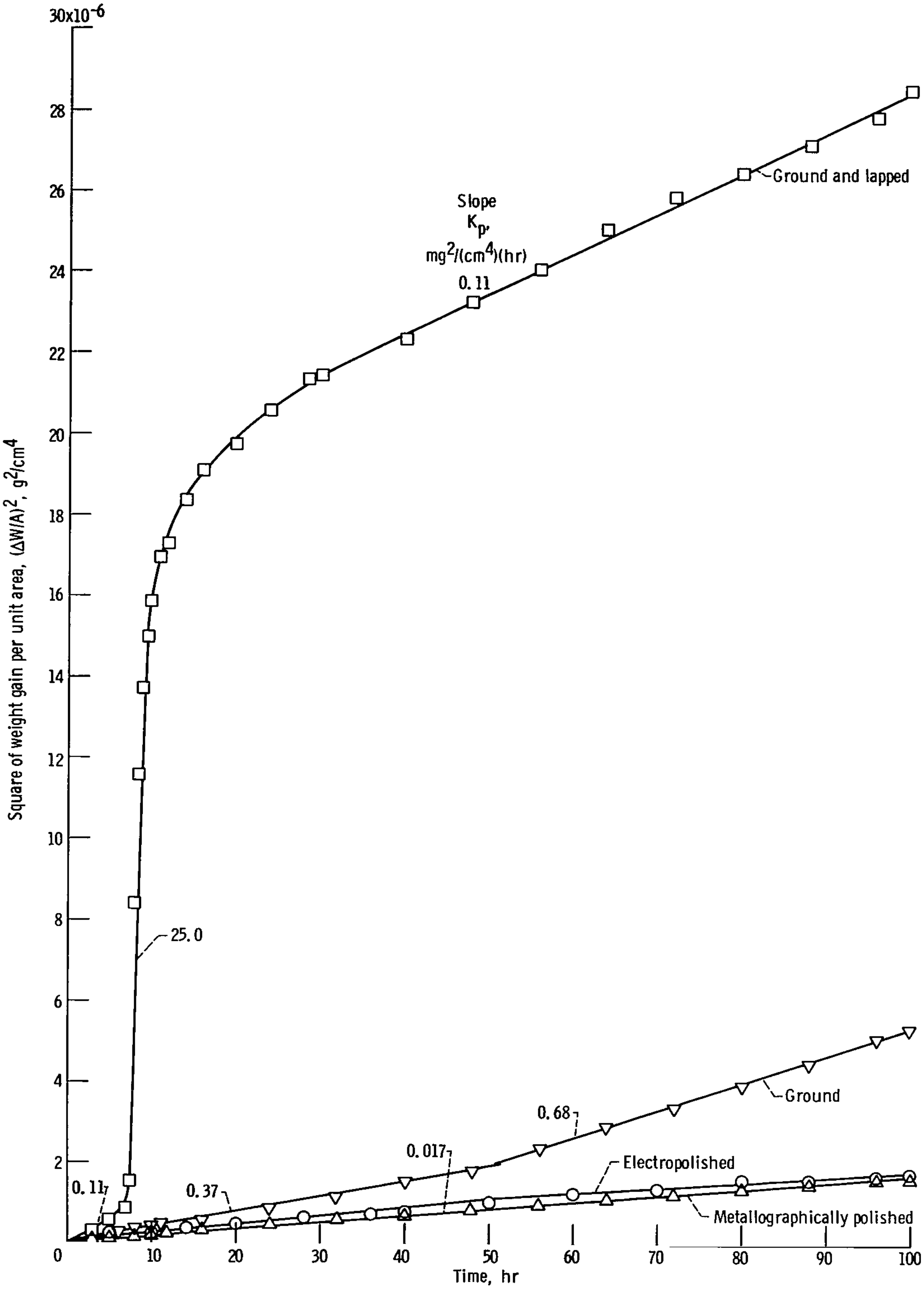

Figure 5. - Effect of surface preparation on weight gain of WI-52 during oxidation in air at 1800° F (1255 K).

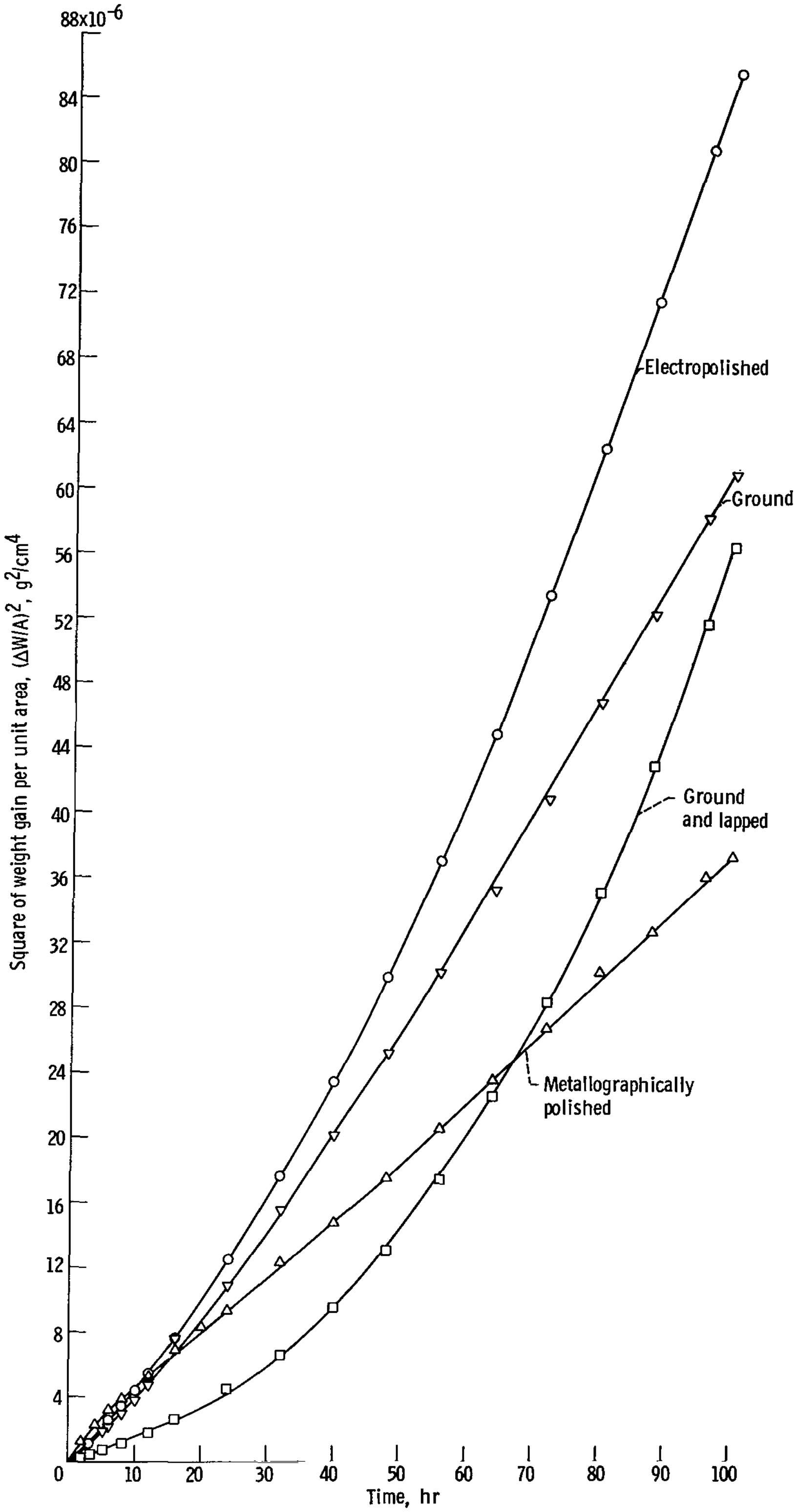

Figure 6. - Effect of surface preparation on weight gain of WI-52 during oxidation in air at 2000° F (1366 K).

HTXRD (see the following subsection), we know that Cr_2O_3 is the predominant phase at this point. During the "anomalous weight increment," the rate increases to a maximum of over 10 $mg^2/(cm^4)(hr)$. This rate is about the value Phalnikar (ref. 7) gave for Co - 14 percent Cr and Kofstad (ref. 5) gave for about Co - 20 percent Cr. The final segment of the curve approaches the same rate as the first segment. This is the same observation made by Wolf and Sandrock (ref. 4).

Neither the metallographically polished nor electropolished samples spalled at all, while the ground samples spalled in some areas and the ground-and-lapped sample spalled drastically. Figure 7 shows a macrophotograph of the polished and the ground-and-lapped samples after 100 hours exposure in air at 1800° F (1255 K). The surface of the metallographically polished sample is smooth, while the ground-and-lapped sample is pockmarked from the spalling process. This photograph was taken 20 minutes after the latter sample was removed from the furnace and while it was still spalling. In this, as in all other cases of spalling of WI-52, spalling does not start until the sample is below red heat, ≈800° F (700 K), and continues for over 24 hours.

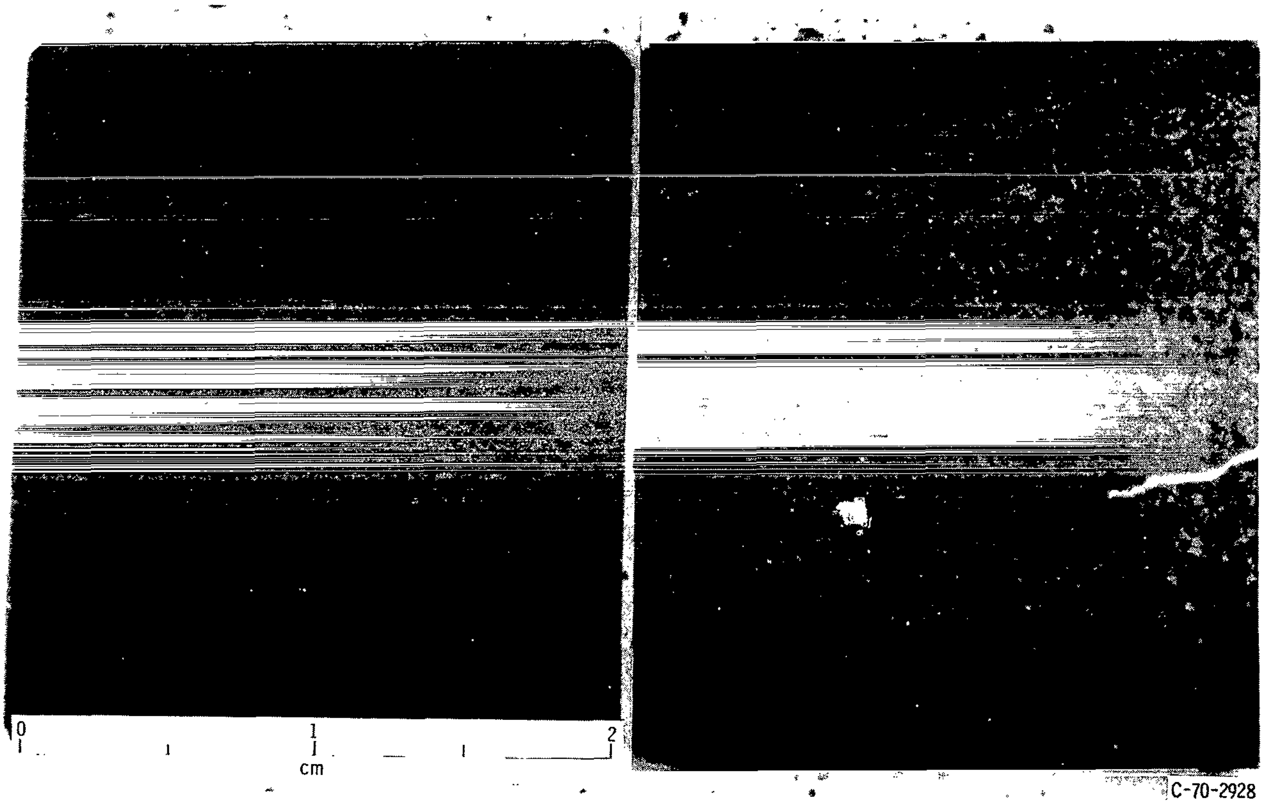

(a) Polished.

(b) Ground and lapped.

Figure 7. - Effect of surface preparation on spalling of WI-52 after 100 hours in air at 1800° F (1255 K). Spalling of ground-and-lapped sample was still occuring while photograph was being made (~20 min after removal from furnace).

Because of this long time effect, suggesting a phase transformation, and the fact that spalling only occurred on samples which formed CoO on the surface, spalling is probably due, at least in part, to the formation of Co_3O_4 from oxygen-saturated CoO upon cooling. At temperatures above 1700° F (1200 K), only CoO is stable, but it can dissolve much more oxygen than at lower temperatures (ref. 8). As CoO is cooled, Co_3O_4 is formed both by oxidation of CoO at the gas-oxide interface and precipitation from the supersaturated CoO within the oxide grains. The oxidation can be prevented by cooling rapidly or under inert gas, but the precipitation cannot be prevented by either technique (ref. 8, p. 268). As this precipitation is accompanied by a 6-percent volume contraction and can take place at relatively low temperatures where oxide plasticity is low, considerable strain may be set up in the oxide and could contribute greatly to spalling.

At 2000° F (1366 K), several factors conspire to make the weight-gain data difficult to evaluate. One of the most important is the volatility of Cr_2O_3 in air (ref. 9). Thus, samples forming the greatest amounts of Cr_2O_3 will show lesser amounts of oxidation by ΔW measurements than actually occur. The volatility of $CoCr_2O_4$ has not been well established, but it is probably an important factor. In addition, the relative importance of the grain-boundary and matrix oxidation may change. Certainly there is more intergranular oxidation at 2000° F (1366 K) than at 1800° F (1255 K).

The weight-gain curves at 2000° F (1366 K) for the different surface preparations do not show the same relations as shown at 1800° F (1255 K). At the end of 100 hours, the metallographically polished sample still shows the lowest weight gain, but the electropolished sample is not similar to it. Indeed the electropolished sample shows the highest gain of any of the samples tested. The ground and the ground-and-lapped samples fell in between. As previously noted, the ΔW values are suspect because of oxide volatility, and certainly the electropolished sample, in which the grain-boundary carbides may be left in relief by the polishing operation, is more susceptible to intergranular attack than the others. Also, slight overetching, which is difficult to control, can lead to a reduction in Cr content in the matrix and a subsequent drastic increase in oxidation rate. The oxidation rates of all samples at 2000° F (1366 K) are within a factor of 3 of the rate for Co-20Cr as measured by Phalnikar (ref. 7), but more than 100 times slower than that of Kofstad (ref. 5). For example, the average rate for the metallographically polished sample is 0.38 $mg^2/(cm^4)(hr)$ as compared to 0.6 to 1.0 $mg^2/(cm^4)(hr)$ for Phalnikar's samples, and about 60 $mg^2/(cm^4)(hr)$ for those of Kofstad. All samples run at 2000° F (1366 K) spalled on cooling.

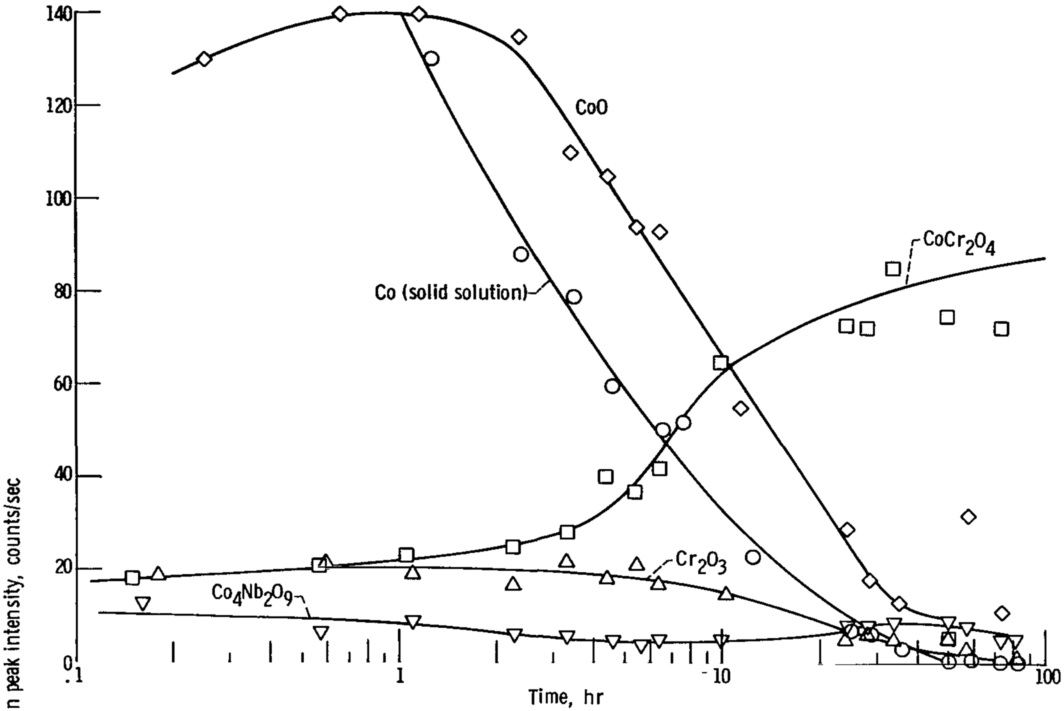

(a) Temperature, 1800° F (1255 K).

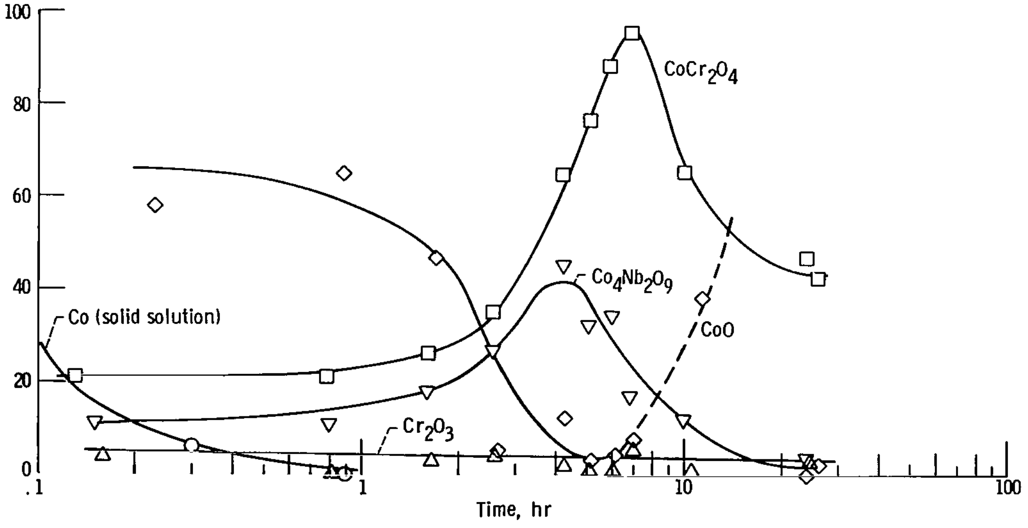

(b) Temperature, 2000° F (1366 K).

Figure 8. - Oxidation of polished WI-52 in air (determined by high-temperature X-ray diffraction).

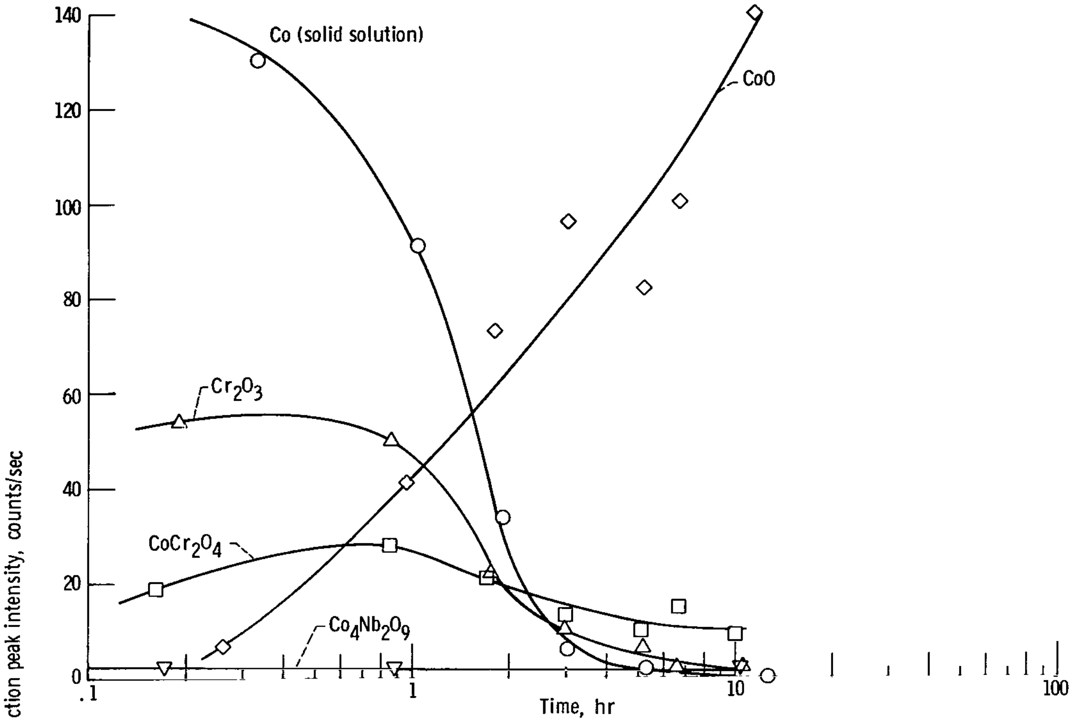

(a) Temperature, 1800° F (1255 K).

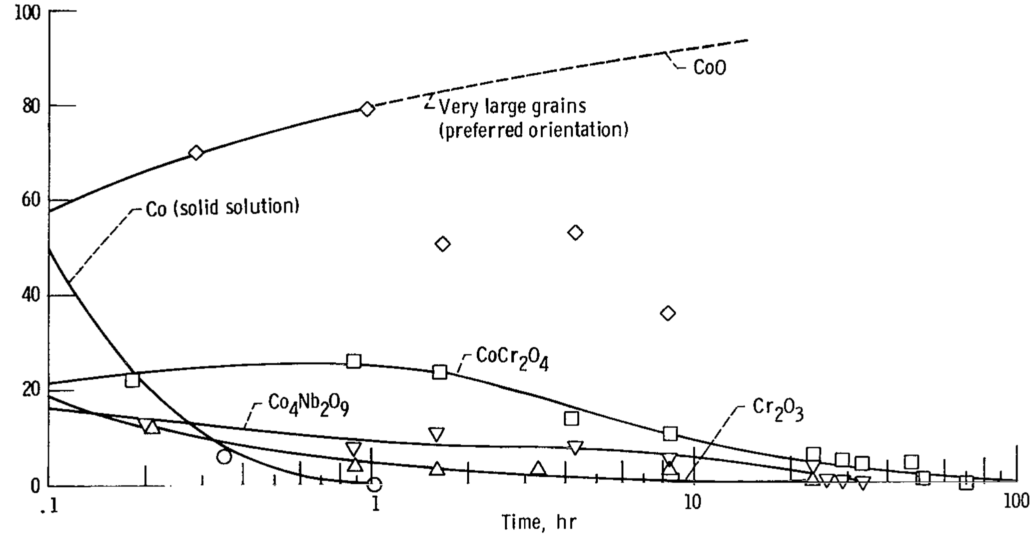

(b) Temperature, 2000° F (1366 K).

Figure 9. - Oxidation of ground-and-lapped WI-52 in air (determined by high-temperature X-ray diffraction).

High-Temperature X-Ray Diffraction (HTXRD)

The results of the HTXRD are covered in detail in reference 3. The pertinent data are shown in figures 8 and 9. As can be seen from these figures, surface preparation strongly influences the order and rates of formation of the oxides. Polished surfaces seem to have an initial preponderance of CoO with some Cr_2O_3 and $CoCr_2O_4$. This is followed by a rapid increase in $CoCr_2O_4$ at the expense of the other phases. At 1800° F (1255 K), nothing further occurs; but at 2000° F (1366 K), this sequence is followed by a resurgence of CoO.

The data for ground-and-lapped specimens indicate an initial large amount of Cr_2O_3 followed by rapid growth of CoO at 1800° F (1255 K). This is probably also the case at 2000° F (1366 K), but the reaction is so rapid that only the tailoff of the Cr_2O_3 can be seen at short times.

Room-Temperature X-Ray Diffraction (XRD)

Table II contains the results of room-temperature XRD. In general, the phases were those expected from the data from HTXRD. However, Co_3O_4 and $CoWO_4$ were found by XRD but not by HTXRD. In addition, both $Co(Nb, W)_2O_6$ and $Co_4(Nb, W)_2O_9$ were found. This was anticipated from the HTXRD results, but not demonstrated by them. The presence of Co_3O_4 at room temperature indicates that the CoO-Co_3O_4 transformation has been confirmed.

TABLE II. - SUMMARY OF ROOM-TEMPERATURE X-RAY DIFFRACTION

ON WI-52 OXIDIZED FOR 100 HOURS IN AIR

Temperature		Surface	CoO	Co_3O_4	$CoCr_2O_4$	Cr_2O_3	$Co_x(Nb,W)_2O_{5+x}$	$CoWO_4$
°F	K							
1800	1255	Polished	-----	----	Strong	Weak	Very weak	----
		Electropolished	-----	----	Strong	↓	↓	----
		Ground and lapped	Strong	Weak	Medium	↓	↓	Weak
		Ground	Strong	Weak	Medium	↓	↓	Weak
2000	1366	Polished	Strong	Weak	Strong	Medium	Weak	Weak to medium
		Electropolished	↓	↓	↓	↓	↓	↓
		Ground and lapped	↓	↓	↓	↓	↓	↓
		Ground	↓	↓	↓	↓	↓	↓

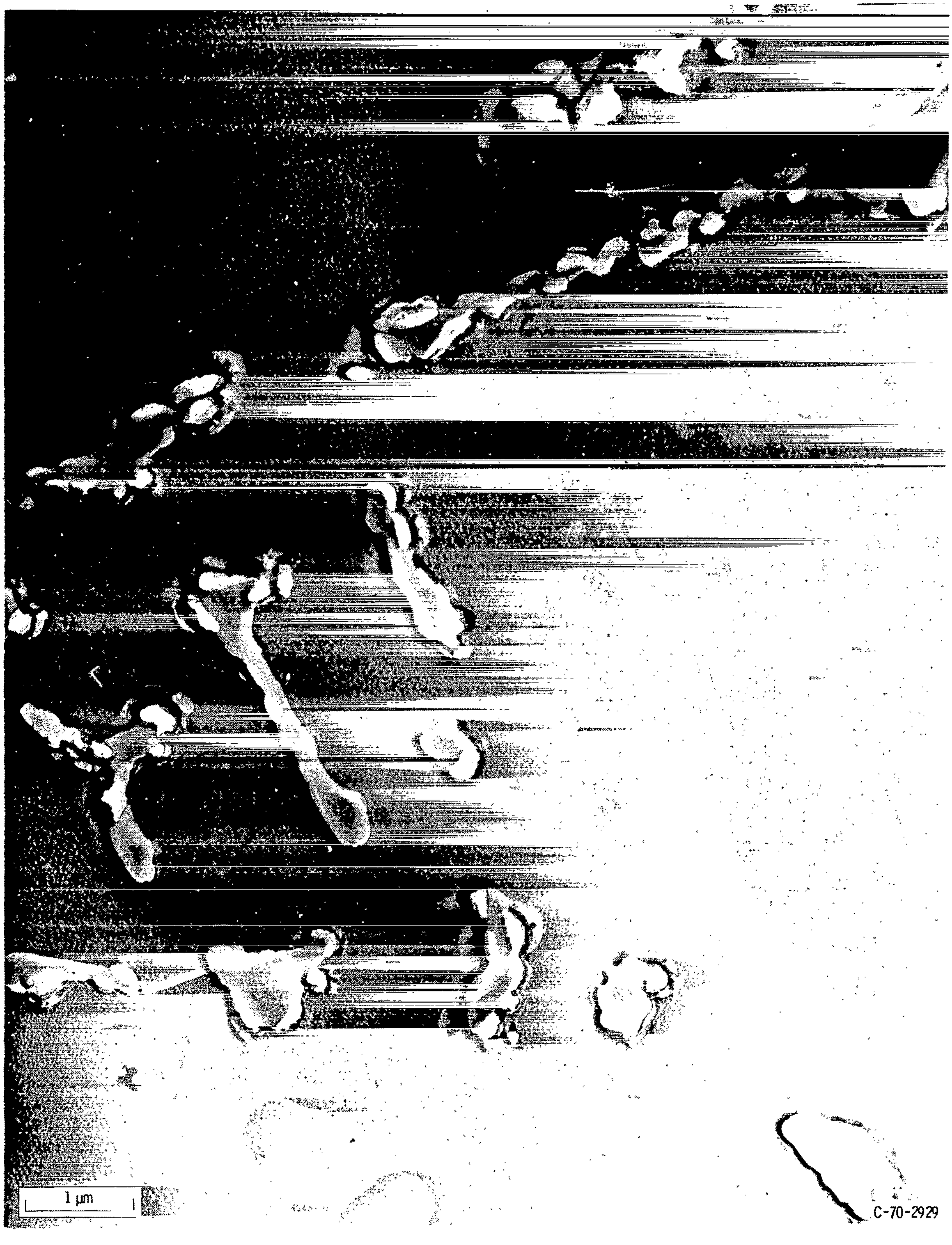

Figure 10. - Onset of oxidation of WI-52 in air. Electron micrograph after 2 minutes at 2000 ° F (1366 K). X18 200.

Room-Temperature Metallography

Room-temperature electron metallography was used in an attempt to confirm the details of the initial oxidation of the (Nb, W)C. Samples of polished WI-52 were oxidized for 2 and 4 minutes at 2000° F (1366 K). Upon cooling, replicas of the surface were made and compared to those of unoxidized samples in the electron microscope. The 2-minute specimen (fig. 10) showed oxide growth on the (Nb, W)C and the 4-minute specimen showed that this had proceeded further. In fact, much of the newly formed oxide adhered to the replica of the 4-minute specimen. Electron diffraction of the extracted material gave a Nb_2O_5 pattern.

To find out what happened to the W present in the carbide, the (Nb, W)C was extracted from the as-cast WI-52. The extract was subsequently oxidized for 4 minutes at 2000° F (1366 K). While the oxidized product was again found to be Nb_2O_5 by XRD, XRF determined that the Nb-to-W ratio was the same before and after oxidation even though no trace of a carbide was left. Apparently the W can substitute for Nb in Nb_2O_5.

Metallography was hampered by severe spalling of some of the samples oxidized at 1800° F (1255 K) and all of the samples oxidized at 2000° F (1366 K). This problem was alleviated with varying degrees of success by the slow cooling of the HTXRD samples and the potting of the ΔW samples.

Figures 11(a) to (c) show the microstructures of the ground, ground-and-lapped, and polished ΔW samples after 100 hours at 1800° F (1255 K). All three are shown without potting in metal. Some spalling had occurred in the ground sample, much spalling had occurred in the ground-and-lapped specimen, but little spalled from the polished sample. The polished sample has a nearly continuous layer of spinel which probably accounts for its nearly parabolic weight-gain curve. Between the spinel and the metal is a thin layer of Cr_2O_3, visible only under polarized light with its characteristically green color, and beneath this can be seen the intergranular attack. The ground-and-lapped sample shows pockets of spinel left after spalling. It too has a thin Cr_2O_3 layer underlying the spinel. The ground sample is similar to the ground-and-lapped sample. Note that while the ground-and-lapped and polished samples had about the same amount of intergranular attack, the ground sample showed less than either.

At 2000° F (1366 K) the picture changes in the rapidity of the reactions (see figs. 12(a) and (b)). After 100 hours the polished sample (fig. 12(a)) has an overlayer of CoO and the innermost scale layer is a mixed layer of Cr_2O_3 and spinel. It also has more severe intergranular attack. The ground sample (fig. 12(b)), which has spalled, shows an interesting sequence, apparent under polarized light, of metal with intergranular oxidation, thin Cr_2O_3, spinel, thin Cr_2O_3, crack, thin Cr_2O_3, spinel, and CoO. At this temperature the intergranular attack is the same for both surface preparations.

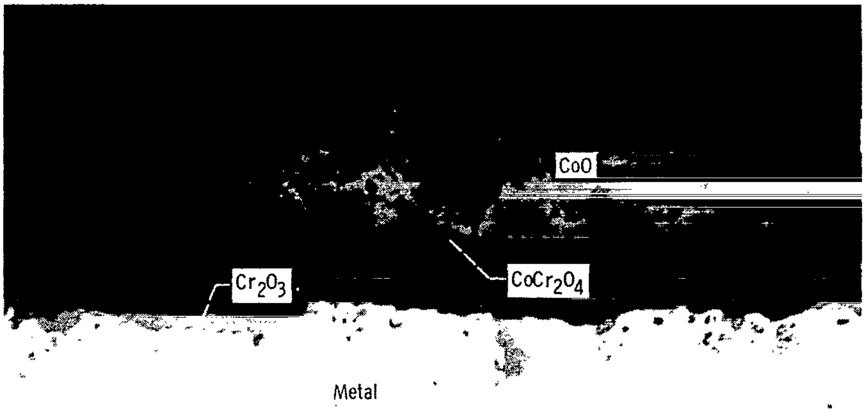

(a) Ground.

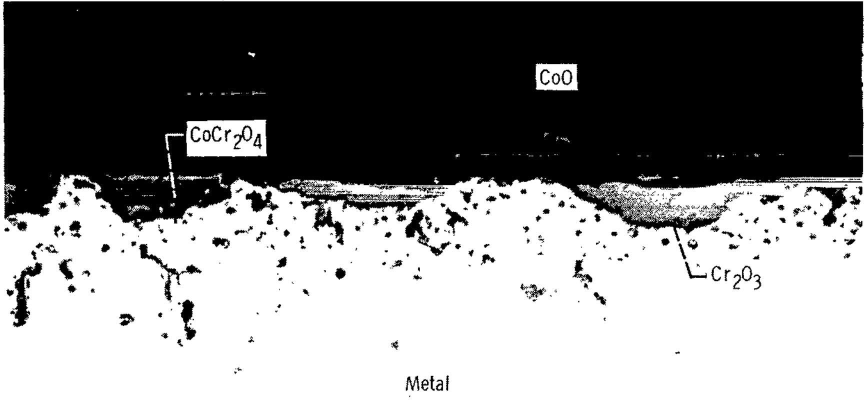

(b) Ground and lapped.

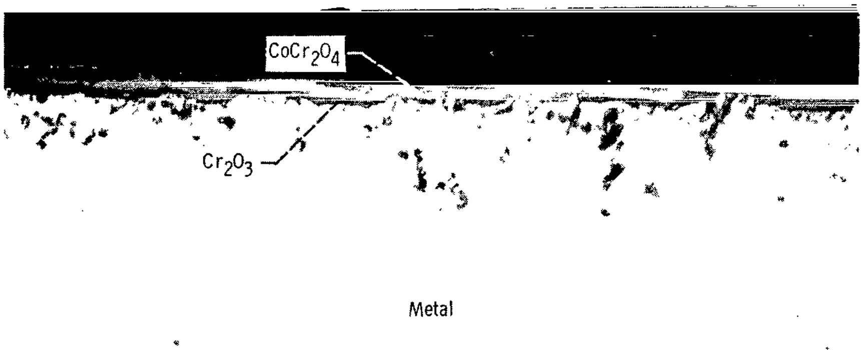

C-70-2930

(c) Polished.

Figure 11. - Metallography of WI-52 oxidized at 1800° F (1255 K) in air for 100 hours. X500.

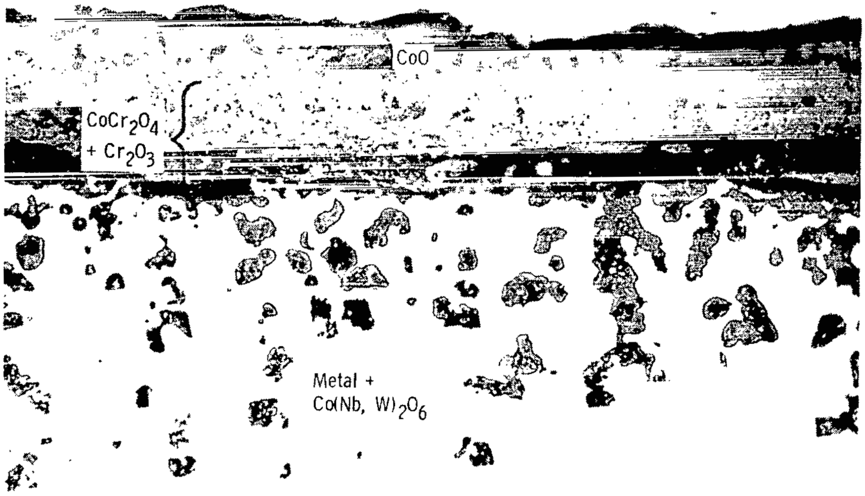

(a) Polished.

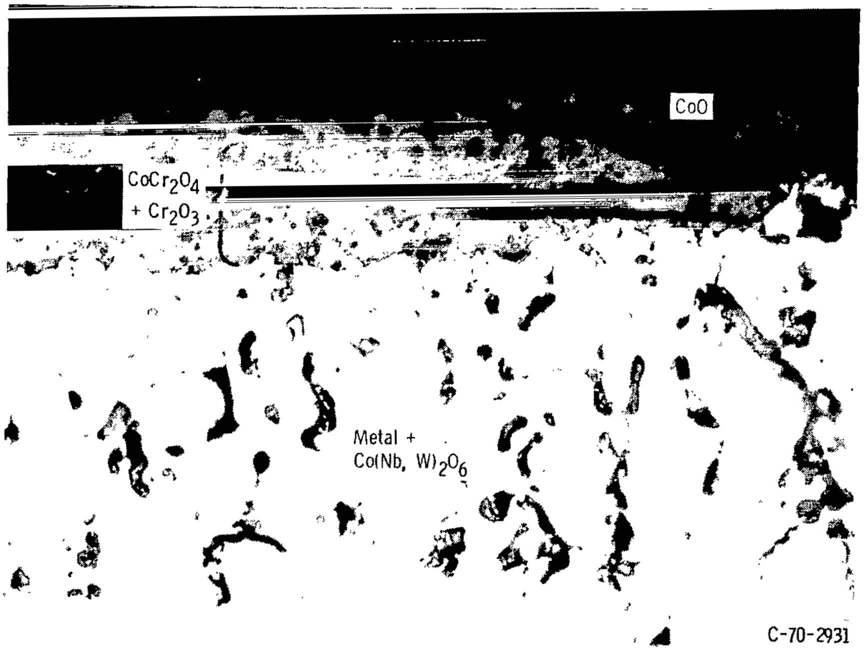

(b) Ground.

Figure 12. - Metallography of WI-52 oxidized at 2000° F (1366 K) in air for 100 hours. X500.

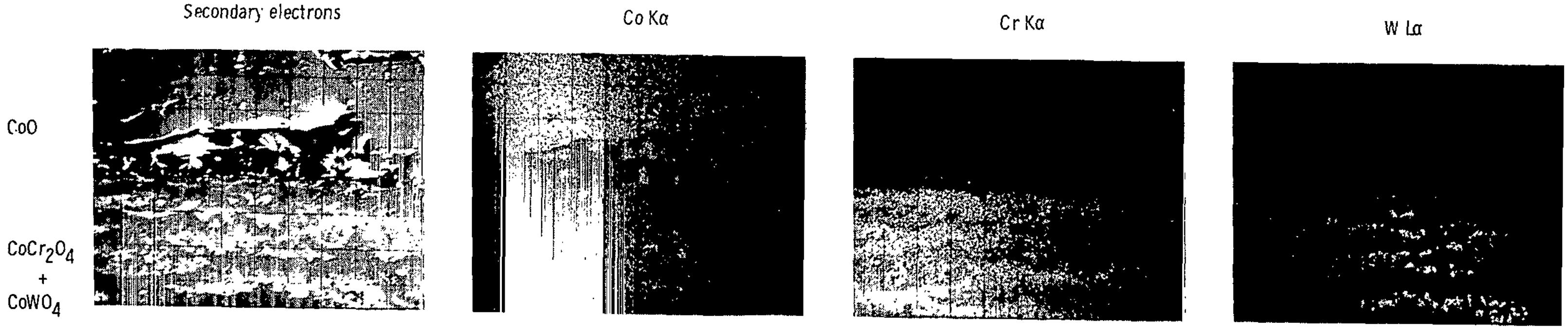

(a) Outermost scale.

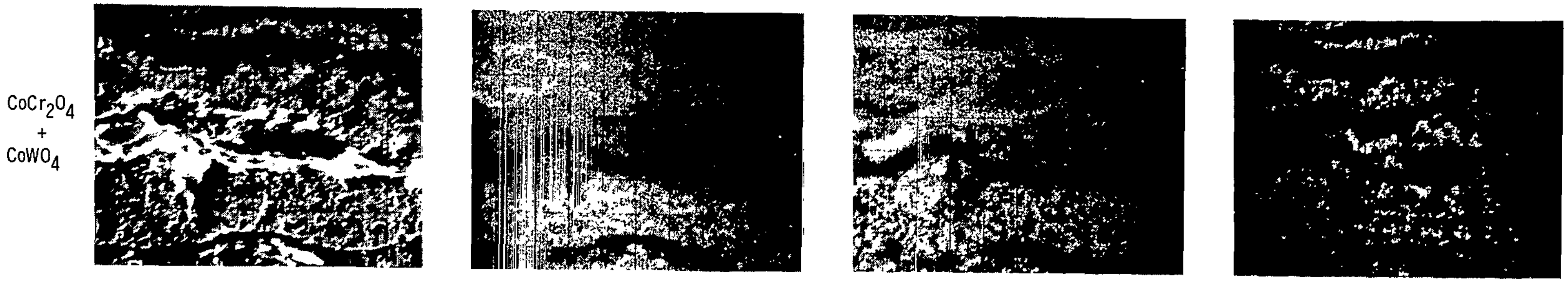

(b) Intermediate scale.

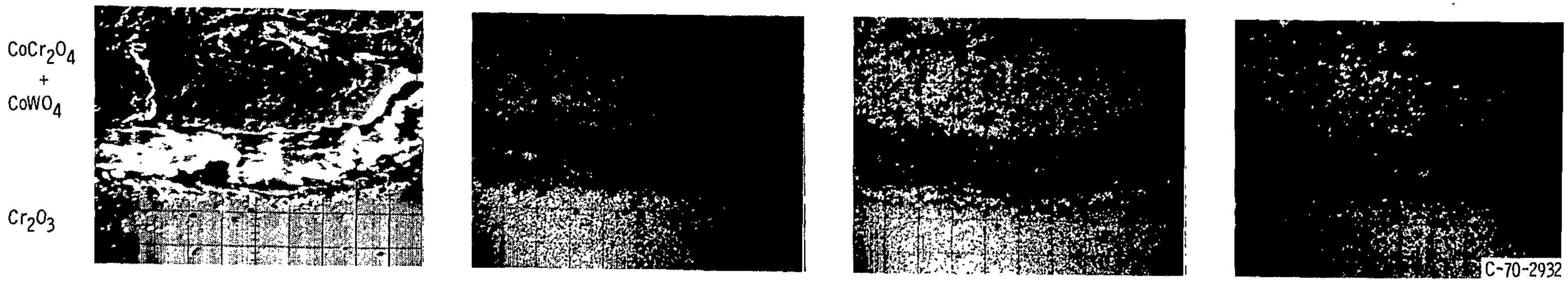

(c) Scale adjacent to metal.

Figure 13. - Electron-microprobe fluorescent X-ray images of WI-52 ground and lapped, and oxidized at 2000° F (1366 K) in air for 100 hours. X200.

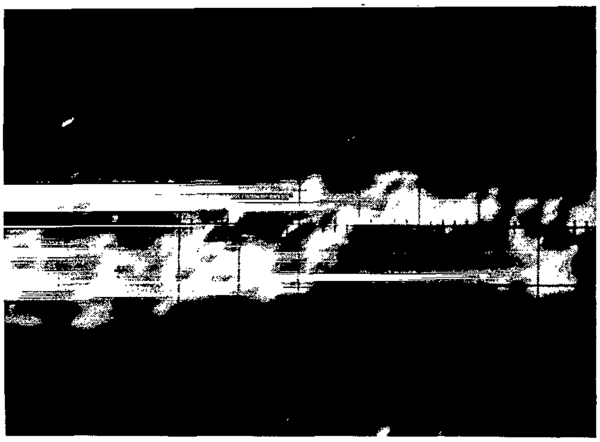

Secondary electrons.

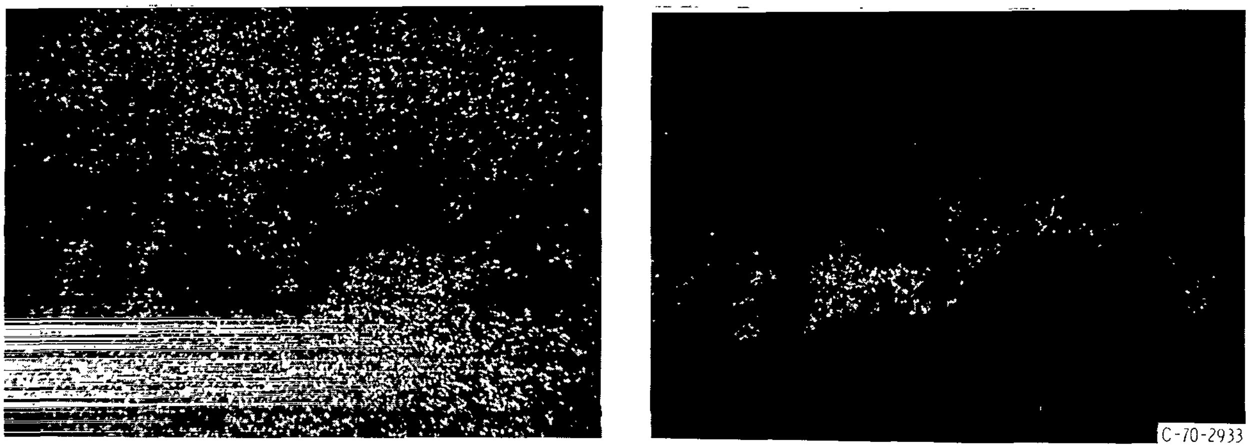

Cr Kα.

W Lα.

Figure 14. - Enlargement of top part of figure 13(b). Electron-microprobe flourescent X-ray images of WI-52 ground and lapped, and oxidized at 2000° F (1366 K) in air for 100 hours. X1000.

Electron Microprobe (EMP)

To supplement the metallography, EMP and XRD were used. Figure 13 shows the results of EMP on a ground-and-lapped 2000° F (1366 K) HTXRD sample. In this figure, the outermost scale is shown at the top and that adjacent to the metal at the bottom. Here the slow cooling has retained the scale fairly well even though it has cracked severely during cooling. X-ray raster scans for Co, Cr, and W were used in determining the distribution of the major oxide phases. They can be summarized as follows:

(1) At the metal-oxide interface is a thin layer rich in Cr but poor in Co and W - probably Cr_2O_3.

(2) The next layer is a mixture of two compositions. One is rich in Cr and poor in W, while the other is rich in W and poor in Cr. The Co is uniformly distributed. These must be $CoCr_2O_4$ and $CoWO_4$.

(3) Then follows a region whose composition is similar to (2), but which is layered. Figure 14 shows this area in greater detail to clarify the relation between the Cr and W.

(4) Finally a region with only Co, most likely CoO.

Scans of Fe and Nb showed no particular concentrations of these elements.

High-Temperature Metallography (HTM)

The HTM results show that the sequence of oxidation may be broken into several consecutive stages (see figs. 15 and 16). Initial oxidation occurs at the grain boundaries as noted by the darkening of the carbide platelets (compare fig. 15(a) with fig. 1). This reaction is

$$2(Nb,W)C + 3\frac{1}{2} O_2 \rightarrow (Nb,W)_2O_5 + 2CO \qquad (1)$$

It should also be noted at this stage (fig. 15(a)) that the $(Cr,Co,W)_6C$ has reacted slightly to show pale gray irregular shapes (again compare with fig. 1). From subsequent behavior it may be inferred that these are areas of Cr_2O_3 formation.

The next stage (fig. 15(b)) also involves the grain-boundary material. This stage includes the reaction of the $(Nb,W)_2O_5$ with the adjacent matrix and oxygen to form the oxide found in the HTXRD results:

$$(Nb,W)_2O_5 + Co + \frac{1}{2} O_2 \rightarrow Co(Nb,W)_2O_6 \qquad (2)$$

(a) Time, 20 seconds.

(b) Time, 96 seconds.

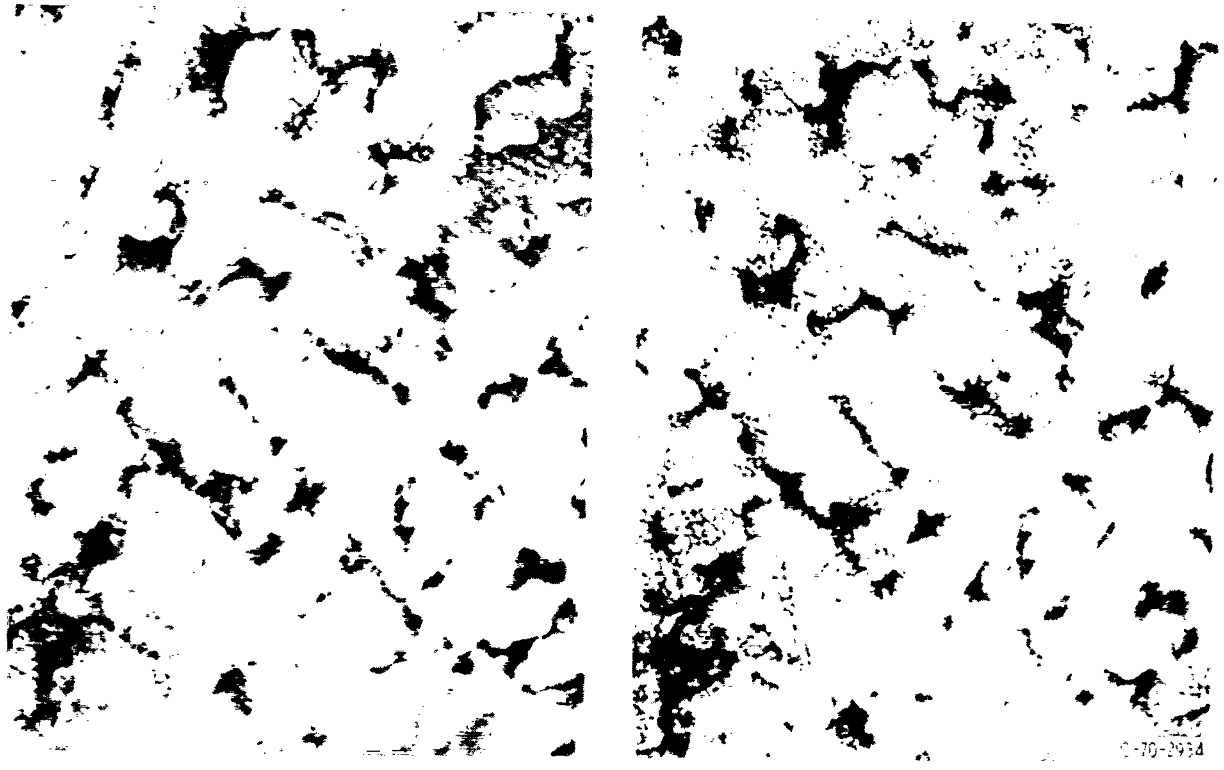

(c) Time, 101 seconds.

(d) Time, 9 minutes.

Figure 15. - High-temperature microscopy (X325) of polished WI-52 at 2000° F (1366 K) in air. Times are from start of heating. Sample reached temperature at 100 seconds.

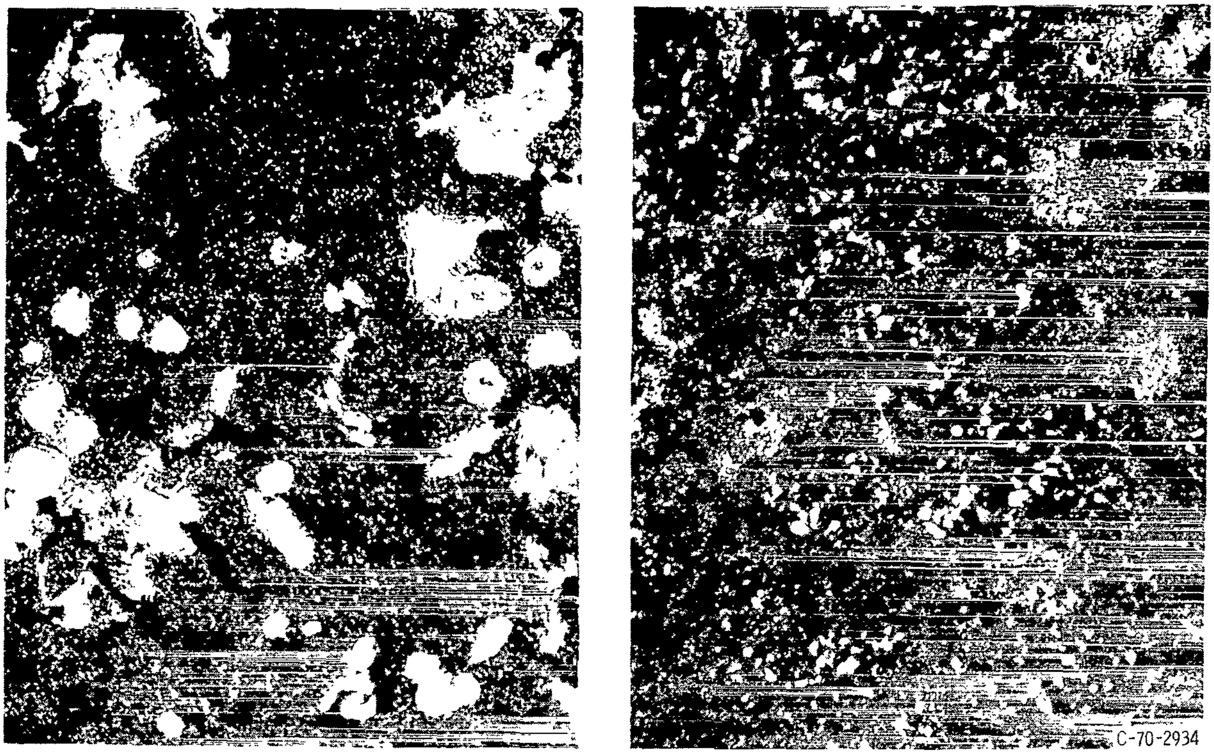

(e) Time, 25 minutes. (f) Time, 150 minutes.

Figure 15. - Concluded.

$$Co(Nb,W)_2O_6 + 3Co + 1\frac{1}{2}O_2 \rightarrow Co_4(Nb,W)_2O_9 \qquad (3)$$

That the reaction does occur in two stages is likely because the product of equation (2) was sometimes found by room-temperature XRD when samples were removed from near the oxide-metal interface.

As these reactions proceed, the matrix begins to oxidize perceptibly in smooth, thin layers. This can be seen as a succession of interference colors that are only suggested in the black-and-white prints (fig. 15(c)). This film is mostly CoO. Note that the oxidized $(Cr,W,Co)_6C$ remains relatively white, indicating the stability of Cr_2O_3. These areas will be the last to change in the next sequence.

Immediately following the CoO formation, little nodules of spinel begin to appear in the center of the CoO (fig. 15(d)). These are quickly augmented with other nodules. This appears to be a nucleation-and-growth formation; however, one-frame-per-second motion pictures taken of this stage seem to indicate that the formation takes place in

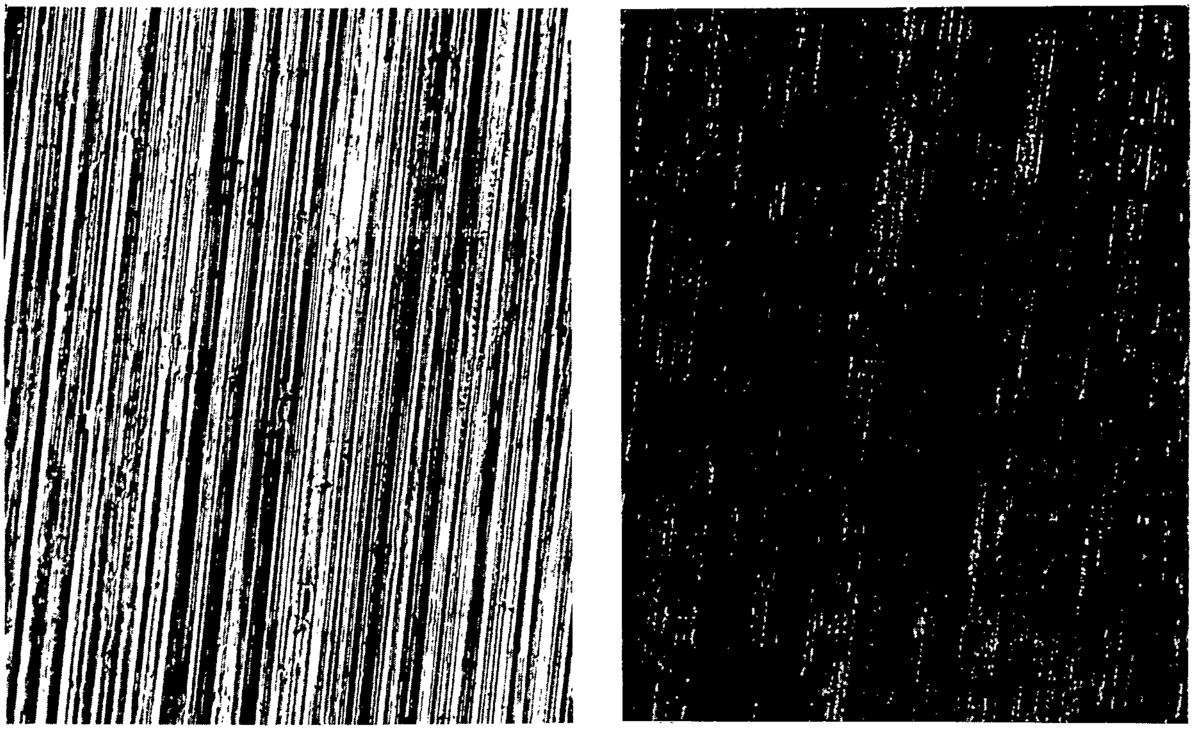

(a) Time, 45 seconds.

(b) Time, 20 minutes.

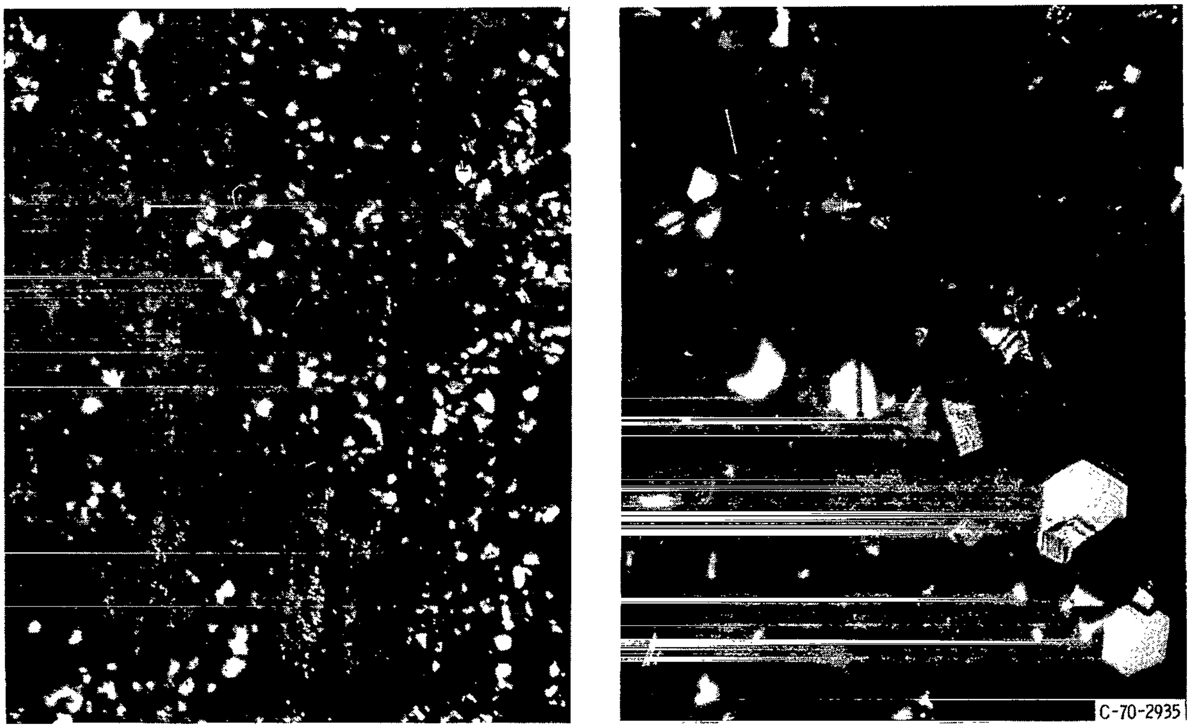

(c) Time, 335 minutes.

(d) Time, 49 hours.

Figure 16. - High-temperature metallurgy of WI-52 with 320-grit surface preparation. Times are from start of heating. Sample reached 2000° F (1366 K) at 100 seconds. X325.

steps. One thing that can be established is that they start at the middle of the CoO areas and grow toward the grain boundaries and are not initiated at the grain boundaries. With time (fig. 15(e)), the growth of the spinel covers the sample completely except for the Cr_2O_3 and $Co_4(Nb,W)_2O_9$. At longer times, the spinel grows over the Cr_2O_3 and partially over the $Co_4(Nb,W)_2O_9$ (fig. 15(f)).

At this point, large cubic crystals of CoO begin to appear at the boundary between the spinel and the $Co_4(Nb,W)_2O_9$. From then on, the growth of CoO continues to spread although individual crystals do not seem to enlarge markedly. With the introduction of the CoO crystals, limited depth of field becomes an increasing problem inasmuch as the crystals grow out making it impossible to focus on both the spinel and the CoO simultaneously. At this point then, the run was terminated.

In order to attempt to see differences in oxidation of WI-52 as a result of surface finish, a sample was observed which had been abraded with 320-grit emery paper (see fig. 16). As in the final frames of the polished sample shown in figure 15, limited depth of field was a problem. Here, however, the scratches made it a problem almost from the beginning. Visual observation was not as severely hampered, since the focus could be changed during viewing, but photography was difficult. Just as the abrading blurred the initial features of the sample, the sequence of events seemed to be blurred. One stage merged into another.

The first frame shows just the surface with its long parallel scratches. The scratches are broken by what appear to be particles of hard carbides. As the sample heats up, Cr_2O_3 forms preferentially along the scratches. This kind of Cr_2O_3 formation was seen by Grisaffe and Lowell (ref. 10) in several other superalloys. At the same time, $Co_4(Nb,W)_2O_9$ is being formed, apparently underneath the Cr_2O_3. Some spinel is probably also present (ref. 3), but Cr_2O_3 predominates. Soon after, large CoO crystals start to grow. Again as in the polished sample, they appear to start at the $Co_4(Nb,W)_2O_9$-matrix interface, but this is not conclusive because of the smearing. With time, the CoO grows quite large, although following this growth is difficult, once again because of the depth of field involved. Visual examination seemed to indicate that the grains of CoO sometimes got smaller with time, but this could not be definitely established. If true, it might indicate a reaction of CoO with Cr_2O_3 (solid or gaseous).

Proposed Oxidation Models

As can be seen from the preceeding results, any model for WI-52 oxidation which does not take into account the state of the surface prior to oxidation is meaningless. Ideally, the unreacted surface would be completely characterized, including such things as a low-energy electron-diffraction analysis of the oxide surface film. The models presented here will be restricted to an assumption, perhaps false, that the oxide layer present at the start of oxidation is only a few atom layers thick. Variables associated with this thin layer and its composition will not be discussed. These models are shown schematically in figure 17 and will be described individually.

The mode of oxidation for polished surfaces of WI-52 has many stages but is clearer than that of distressed surfaces. Stage 1 (fig. 17(a)) shows the metal-gas interface upon insertion of the sample into the furnace. Stage 4 is generally completed before the sample reaches the test temperature. Stages 2, 3, and 4 consist of initial oxidation of the grain-boundary carbides followed by the reaction of this product with the matrix and subsequently by the formation of CoO over the matrix and Cr_2O_3 over the $(Cr, W, Co)_6C$. Whether there is any Cr_2O_3 underlying the CoO is hard to say; but if it is present, it is there in very small amounts. Stages 5 and 6 are the nucleation and growth of $CoCr_2O_4$, starting near the middle of the matrix grains and working out to cover all but the $Co_4(Nb,W)_2O_9$ and the Cr_2O_3 over the $(Cr, W, Co)_6C$. These stages are followed by further growth of the $CoCr_2O_4$ until it covers nearly the whole surface. Stage 7 represents the oxides after 100 hours at 1800° F (1255 K).

At higher temperatures, or perhaps longer times, the oxidation continues to stages 8 and 9. Stage 8 is the beginning of the formation of CoO at the $CoCr_2O_4$-$Co_4(Nb,W)_2O_9$ interface. The CoO then grows to cover the entire surface. This is accompanied by a change in the solid-solution composition sufficient to allow the formation of $CoWO_4$. After $CoWO_4$ formation has removed sufficient W from the matrix, $CoCr_2O_4$ proceeds. This leads to the alternating layers of $CoWO_4$-$CoCr_2O_4$ found by the microprobe.

There seem to be fewer stages in the ground-and-lapped model, but there are more uncertainties. Stage 1 (fig. 17(b)) also is the surface as inserted into the furnace. While heating to the oxidation temperature, Cr_2O_3 forms preferentially in the stressed areas. That this does occur seems certain (see HTXRD and ref. 10); why it occurs is not at all clear. With time (stage 3), the Cr_2O_3 grows and the (Nb,W)C oxidizes (presumably the $(Cr, W, Co)_6C$ does also; but since it forms Cr_2O_3 anyway, there is no clue as to where, or if, this Cr_2O_3 reacts differently).

The crucial stage is the fourth as this is the onset of the "anomalous weight gain." Cobalt oxide forms very rapidly. The rate at this stage can be explained by assuming the oxidation of a Cr-depleted matrix. This is the rate of a Co - 10-or-15-Cr binary alloy (see ΔW section and refs. 6 and 7). Why this occurs as suddenly as it does is hard to understand. It has been proposed by Wolf and Sandrock (ref. 4) that tearing of the metal from stresses in the oxide opens a greatly enlarged surface area. This explanation was felt necessary because of the very great apparent rates. However, in the case of WI-52, since the rate can be explained by oxidation of a depleted alloy, tearing of the metal is

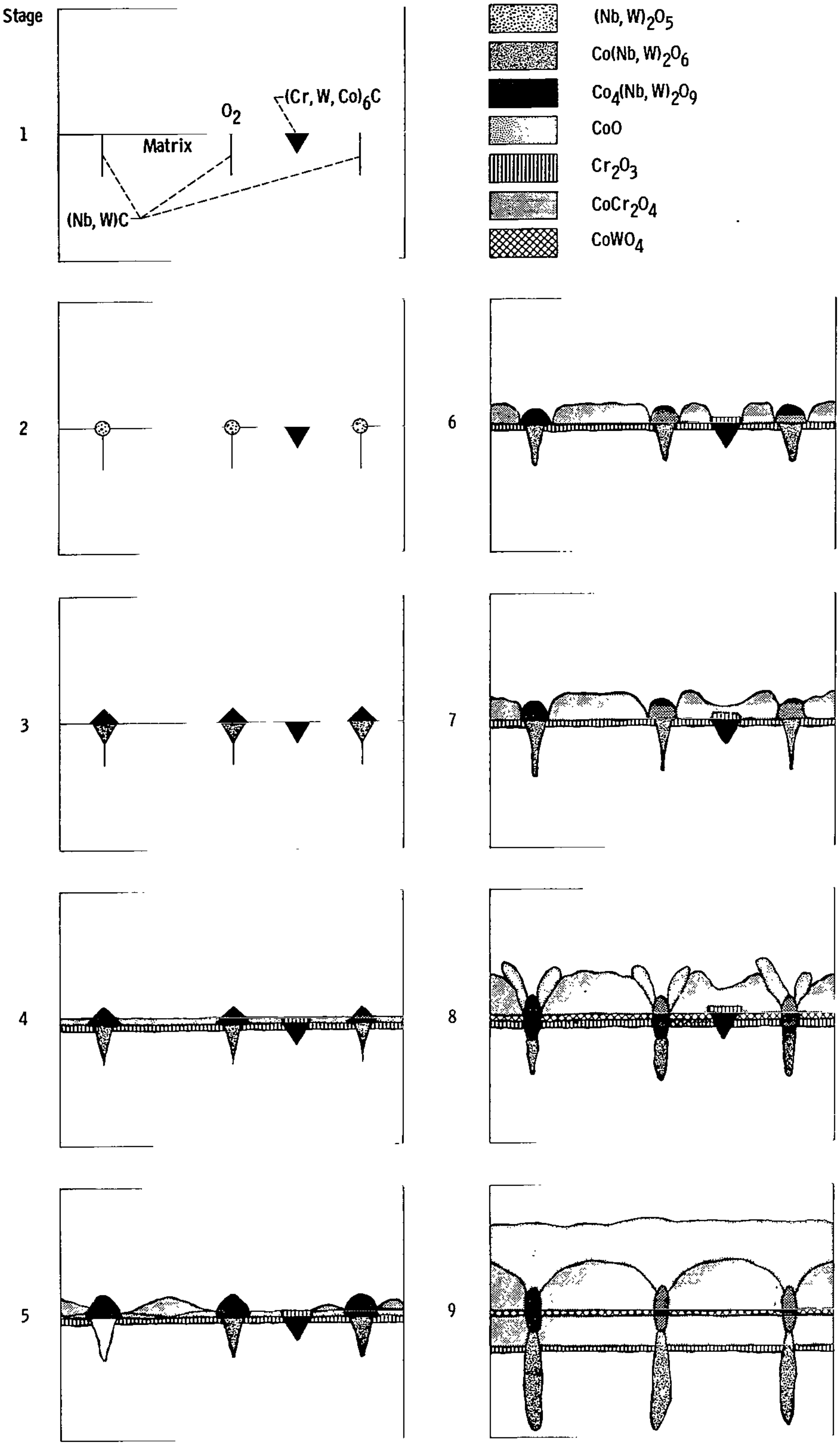

(a) Polished surface.

Figure 17. - Oxidation models for WI-52.

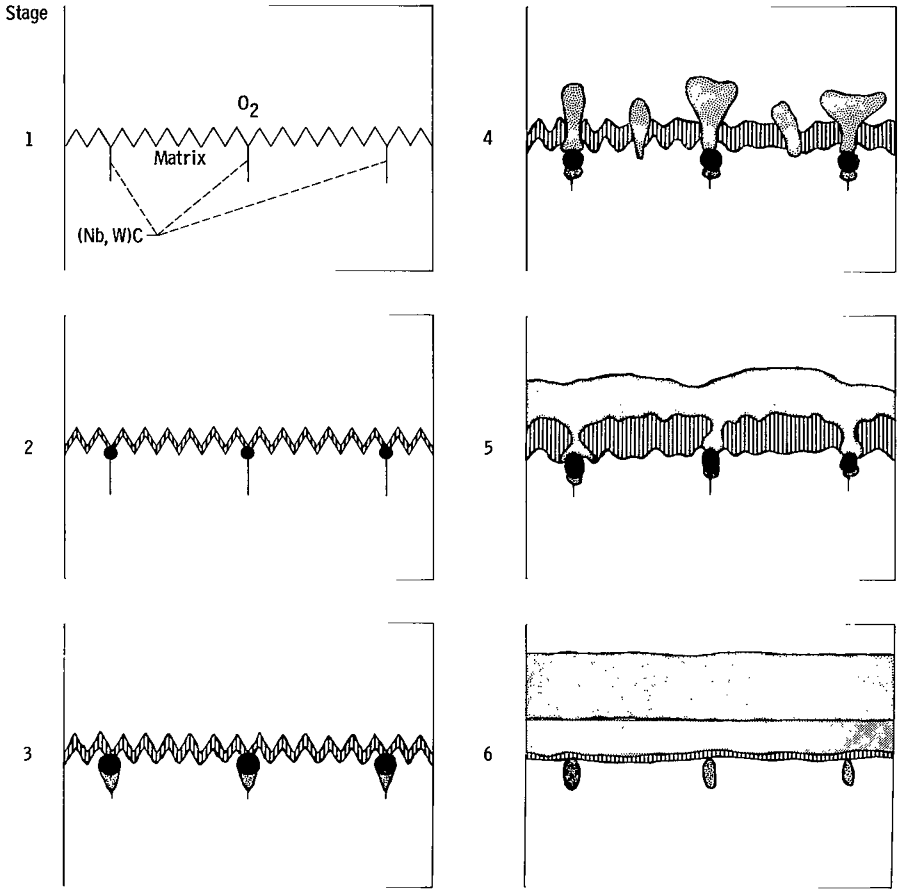

(b) Ground and lapped.

Figure 17. - Concluded.

not a necessary postulate. Perhaps the Cr_2O_3 cracks from growth stresses (ref. 11), combined with paths near the oxidized (Nb,W)C, allow this CoO to form from the depleted substrate. The continuation of the oxidation is just the overgrowth of CoO and subsequent formation of $CoCr_2O_4$ beneath.

CONCLUSIONS

In this attempt to understand the static-air oxidation of WI-52 at 1800° and 2000° F (1255 and 1366 K), high-temperature X-ray diffraction, high-temperature microscopy, and weight-gain experiments were combined. The following results were obtained:

1. Surface preparation is an important variable in the oxidation of WI-52 even at relatively long times (100 hr) and high temperatures.
2. Metallographic polishing promotes the simplest and slowest oxidation on WI-52. This preparation leads to oxidation approaching parabolic. The rates of oxidation for polished samples are near those of Phalnikar, Evans, and Baldwin (ref. 7) of the binary Co-Cr system at comparable Cr contents.
3. At 1800° F (1255 K), the polishing results in a weight gain in 100 hours that is one-fourth that of ground-and-lapped samples. In addition, the polished samples do not spall upon cooling, whereas the ground as well as the ground-and-lapped samples spall.
4. At 2000° F (1366 K), however, the differences in isothermal weight gain are less and all samples spall.
5. The oxidation sequence of polished WI-52 is thought to be as follows:
    - (a) Oxidation of the grain-boundary carbides to $Co_4(Nb,W)_2O_9$ and Cr_2O_3
    - (b) Oxidation of the solid solution to CoO overlaying Cr_2O_3
    - (c) Reaction of the Cr_2O_3 and CoO to form $CoCr_2O_4$
6. The oxidation sequence of ground WI-52 is as follows:
    - (a) Rapid oxidation of the solid solution preferentially to Cr_2O_3, accompained by Cr depletion of the underlying metal
    - (b) Breakdown of the Cr_2O_3 layer followed by very rapid oxidation of the depleted metal underneath to CoO and $CoCr_2O_4$

Lewis Research Center,
National Aeronautics and Space Administration,
Cleveland, Ohio, September 11, 1970,
129-03.

REFERENCES

1. Lund, Carl H.; and Wagner, Herbert J.: Oxidation of Nickel-and Cobalt-Base Superalloys. DMIC Rep. 214, Battelle Memorial Inst., Mar. 1, 1965, p. 14. (Available from DDC as AD-614707.)

2. Douglass, D. L.; and Armijo, J. S.: Improved Oxidation Resistance of Nickel and Cobalt Superalloys. Stanford Research Inst. (NASA CR-94550), Mar. 18, 1968.

3. Lowell, Carl E.; and Drell, Isadore L.: High-Temperature X-Ray-Diffractometer Study of Oxidation of Two Superalloys, WI-52 and IN-100. NASA TM X-2002, 1970.

4. Wolf, James S.; and Sandrock, Gary D.: Some Observations Concerning the Oxidation of the Cobalt-Base Superalloy L-605 (HS-25). NASA TN D-4715, 1968.

5. Kofstad, Per; and Hed, A. Z.: Oxidation Behavior of Co-25Cr and Co-35Cr Alloys. Battelle Memorial Inst. (NASA CR-72420), June 4, 1968.

6. Kofstad, P.; Hed, A. Z.; Wilcox, B.; and Clauer, A.: High Temperature Oxidation of Alloys: Cobalt-Chromium Base Alloys. Battelle Memorial Inst. (NASA CR-90560), Nov. 10, 1967.

7. Phalnikar, C. A.; Evans, E. B.; and Baldwin, W. M., Jr.: High Temperature Scaling of Cobalt-Chromium Alloys. J. Electrochem. Soc., vol. 103, no. 8, Aug. 1956, pp. 429-438.

8. O'Bryan, H. M., Jr.; and Parravano, G.: The Univariant Equilibrium Between the Oxides of Cobalt. Reactivity of Solids. G. M. Schwab, ed., Elsevier Publ. Co., 1965, pp. 256-268.

9. Caplan, D.; and Cohen, M.: The Volatilization of Chromium Oxide. J. Electrochem. Soc., vol. 108, no. 5, May 1961, pp. 438-442.

10. Grisaffe, Salvatore J.; and Lowell, Carl E.: Examination of Oxide Scales in Heat Resisting Alloys. NASA TN D-5019, 1968.

11. Caplan, D.; Harvey, Alma; and Cohen, M.: Oxidation of Chromium at 890° to 1200° C. Corrosion Sci., vol. 3, no. 3, Oct. 1963, pp. 161-175.

NASA-Langley, 1971 —— 17 E-5668

> *"The aeronautical and space activities of the United States shall be conducted so as to contribute . . . to the expansion of human knowledge of phenomena in the atmosphere and space. The Administration shall provide for the widest practicable and appropriate dissemination of information concerning its activities and the results thereof."*
>
> —NATIONAL AERONAUTICS AND SPACE ACT OF 1958

NASA SCIENTIFIC AND TECHNICAL PUBLICATIONS

TECHNICAL REPORTS: Scientific and technical information considered important, complete, and a lasting contribution to existing knowledge.

TECHNICAL NOTES: Information less broad in scope but nevertheless of importance as a contribution to existing knowledge.

TECHNICAL MEMORANDUMS: Information receiving limited distribution because of preliminary data, security classification, or other reasons.

CONTRACTOR REPORTS: Scientific and technical information generated under a NASA contract or grant and considered an important contribution to existing knowledge.

TECHNICAL TRANSLATIONS: Information published in a foreign language considered to merit NASA distribution in English.

SPECIAL PUBLICATIONS: Information derived from or of value to NASA activities. Publications include conference proceedings, monographs, data compilations, handbooks, sourcebooks, and special bibliographies.

TECHNOLOGY UTILIZATION PUBLICATIONS: Information on technology used by NASA that may be of particular interest in commercial and other non-aerospace applications. Publications include Tech Briefs, Technology Utilization Reports and Technology Surveys.

Details on the availability of these publications may be obtained from:

SCIENTIFIC AND TECHNICAL INFORMATION OFFICE
NATIONAL AERONAUTICS AND SPACE ADMINISTRATION
Washington, D.C. 20546